

## Supplementary Information

### Origin of the obliquities of the giant planets by mutual interactions in the early Solar System

The initial conditions for the numerical simulations were generated following closely [S1]: the semimajor axes of the planets were shifted by an amount  $\Delta a$  from the present ones. In all the simulations Jupiter started with  $a_J = 5.45$  AU whereas the semimajor axes of Saturn, Uranus and Neptune were generated at random, within the intervals  $8.38 \leq a_S \leq 8.48$  AU  $9.9 \leq a_U \leq 12$  AU and  $13.4 \leq a_N \leq 17.1$  AU. Those initial conditions where Uranus and Neptune were initially separated in less than 2 AU were discarded, as in [S1]. The orbital eccentricities and inclinations were taken as the present ones, and the longitude of the nodes, the arguments of the perihelion and the mean anomalies were generated at random.

The problem of the integration of the rotational Euler equations is complex and expensive, and requires a very short integration timestep (shorter than the diurnal rotation rate of the planets). For this reason it was not possible for us to simulate the planetary migration in a more realist fashion as in [S1] by N-Body integration of a myriad of planetesimals. Therefore, the semimajor axis of each planet was forced to migrate with a characteristic timescale  $\tau$ , by means of an artificial tangential acceleration applied at each time step  $h$ , of magnitude

$$\Delta \mathbf{v} = \frac{1}{2} \frac{\Delta a}{a} \left(\frac{v_c}{v}\right)^2 e^{-t/\tau} \frac{h}{\tau} \mathbf{v},$$

where  $v$  is the orbital velocity of the planet and  $v_c$  the circular velocity at the distance of the planet. This migration strategy was first introduced in [S2].

The characteristic time scale of migration  $\tau$  was distributed at random, within the interval  $10^6 \text{ yr} \leq \tau \leq 10^7 \text{ yr}$ , with an uniform probability distribution, and the numerical integration was executed for a time span of  $10\tau$ .

The disk, although not physically present in our simulations, should also act damping the eccentricities of the planetary orbits through Dynamical

Friction [S3,S4]. We note that without this effect, the planets end-up with relatively large orbital eccentricities, not consistent with the results shown in figure 1 of [S1], where it is evident that the timescale of eccentricity damping is at least one order of magnitude shorter than the timescale of orbital migration, (consistent with the predictions of the theory of planet-disk interaction [S3,S4]). We modeled this effect as follows: If  $\theta$  is the angle between the instantaneous orbital velocity vector and the direction perpendicular to the radius vector, at each time step  $h$ , we reduced  $\theta$  by

$$\Delta\theta = \frac{\theta}{\tau_e}h,$$

where  $\tau_e$  is the eccentricity damping time scale, on which the orbit becomes perfectly circular. This strategy does not affect the semimajor axis of the planets. In all our simulations  $\tau_e = \tau/10$ . This forced circularization was introduced only if the planets were assumed immersed in the planetesimal disk, that was supposed to start just beyond the initial orbit of the outermost planet. The orbital evolutions obtained in this way were similar to the ones shown in figure 1 of [S1].

The equations of motion for the planet spin-axis vector,  $\mathbf{s}$ , were split into two components: The solar component, and a component arising from the mutual interaction of the planets. The solar component was modeled as in [S5], but in our simulations the orbits of the planets were numerically integrated simultaneously with the rotational equations. For the mutual planetary component, we used the Euler equations of rotation [S6], where the torque  $\mathbf{T}_{ij}$  exerted by the planet  $i$  over the planet  $j$  was computed as [S6]

$$\mathbf{T}_{ij} = \frac{3GM_i}{r^5} \mathbf{r} \times (\mathbf{I} \mathbf{r}),$$

where  $\mathbf{r}$  is the position vector of planet  $i$  in a reference frame with origin at the center of mass of planet  $j$ , coincident with its principal axes of inertia. Therefore  $\mathbf{I}$ , the inertia tensor, is reduced to a diagonal matrix. In addition we have assumed that the planets are oblate spheroids. The vector sum of the total rotational *angular momentum* has to be conserved, and we have tested this conservation during the runs, to ensure the precision of the simulations. The relative error was always better than  $10^{-8}$ .

One of the main quantities determining the evolution of the obliquity of an oblate planet is its precession constant  $\alpha$ , defined by [S7]

$$\alpha = \frac{3 n^2 J_2 + q}{2 \Omega \lambda + l},$$

where  $n$  is the orbital mean motion and  $\Omega$  is the diurnal rotation rate,  $J_2$  is the coefficient of the quadrupole moment of the planet gravity field and  $\lambda$  is its moment of inertia.  $q$  and  $l$  account for the fact that a fraction of the external torque is exerted on the satellite system of the planet, rather than directly on the planet itself [S7]. We adopted for the precession frequencies of each planets the following values, taken from [S7]

$$\begin{aligned} \alpha_J &= (0.077 Myr)^{-1} \\ \alpha_S &= (0.26 Myr)^{-1} \\ \alpha_U &= (4.6 Myr)^{-1} \\ \alpha_N &= (17.6 Myr)^{-1} \end{aligned}$$

Most close encounters in the simulations occur during the first million of years. We recorded usually tens of encounters between Saturn and Uranus, closer than 1 AU (The mutual Hill's radius of Uranus and Neptune, placed at 10 AU is 0.48 AU). Encounters between these two planets as close as  $10^{-2}$  AU are not unusual in several runs. These strong close encounters can change the obliquities up to few tens of degrees. In the case of Uranus and Neptune, there are hundreds of encounters closer than 1 AU in all the runs, and some of them can be as close as  $10^{-2} - 10^{-3}$  AU. these strong close encounters can change the obliquity by up to few degrees. The change in Uranus' obliquity during one close encounter with Neptune is shown in figure 1.

During the period of dynamical excitation of the system, where the resonance crossing occurs, the evolution of the obliquities could be considered as a random walk process of successive kicks in obliquity. The r.m.s change in Uranus obliquity, during Uranus-Saturn encounters, is of  $0^\circ.37$ , whereas during each Uranus-Neptune encounter it is of  $0^\circ.14$ .

In the five runs where one of the ice giants is ejected from the solar system, although it leaves a large obliquity ( $\sim 20^\circ - 40^\circ$ ), it is not possible to adventure a conclusion, because these simulations stop well before the evolution was completed (usually well before  $10^6$  yr). In the six runs with final orbital architectures not compatible with the observed outer solar system, we obtained the following obliquity statistics:

$$\begin{aligned}
\epsilon_J &= 2.1 \pm 0.65 \\
\epsilon_S &= 9.5 \pm 3.4 \\
\epsilon_U &= 77.5 \pm 6.8 \\
\epsilon_N &= 53.5 \pm 18.6
\end{aligned}$$

where the  $\pm$  are standard errors. Therefore, although with a large dispersion in the results, Uranus also leaves, in average, the largest obliquity.

In the model explored here, Uranus also experiences close encounters with Saturn. For this reason it ends up with the largest obliquity. Nevertheless, in six of the runs, Neptune gets a large obliquity ( $\geq 45^\circ$ ), and in four, Saturn reaches obliquities of the same order.

## REFERENCES

- [S1] Tsiganis, K. Gomes, R. Morbidelli, A. and Levison, H. F. Origin of the orbital architecture of the giant planets of the Solar System. *Nature* **435**, 459-461 (2005).
- [S2] Malhotra, R. The origin of Plutos' orbit: Implications for the solar system beyond Neptune *Astron. J.* **110**, 420-432 (1995).
- [S3] Ward, W. R. On disk-planet interactions and orbital eccentricities. *Icarus* **73**, 330-348 (1988)
- [S4] Artymowicz, P. Disk-satellite interaction via density waves and the eccentricity evolution of bodies embedded in disks. *ApJ* **419**, 166-180 (1993).
- [S5] Ward, W. R. Present obliquity oscillations of Mars: Fourth-order accuracy in orbital  $e$  and  $I$ . *JGR* **84**, 237-241 (1979).
- [S6] Danby, J. M. A. *Fundamentals of Celestial Mechanics* (Willmann-Bell, Inc. Richmond, Virginia. U. S. A. 1992).
- [S7] Ward, W. and Hamilton, D. P. Tilting Saturn I. Analytic model. *AJ* **128**, 2501-2509 (2004).
- [S8] Tremaine, S. On the origin of the obliquities of the outer planets. *Icarus* **89**, 85-92 (1991).

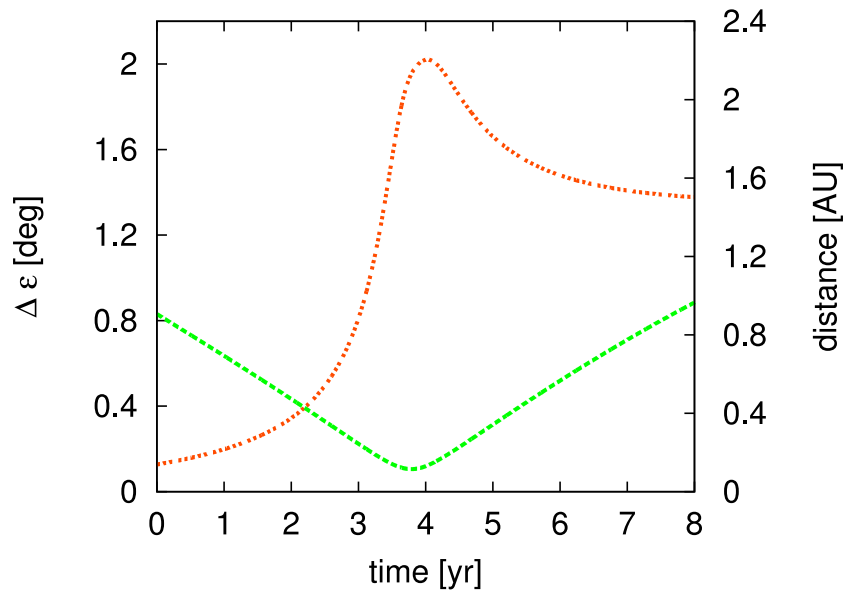


Figure 1: The change in Uranus' obliquity during a close encounter with Neptune. In this encounter, the Uranus-Neptune distance (green curve) gets as close as 0.18 AU. The obliquity variation (red curve) have a maximum during the closest approach, and finally Uranus leaves the encounter with a net obliquity variation of  $\sim 1^\circ.5$ .